



Study of the influence of columns' geometry in hydrodynamic loads

Clemente THM*, Campos NBF†

* *Federal Institute of Education, Science and Technology of Sao Paulo, São Paulo, Brasil*

† *Federal University of Bahia – UFBA, Salvador, Brazil*

Abstract. This work studies the influence that the shape of the section of a column immersed in a watercourse has in relation to the hydrodynamic forces that arise due to fluid-structure interaction. The data about São Paulo state rivers' flows and bridges were revised in order to determine a critical flow rate and choose the cross sections study cases. The simulations made with the ANSYS Fluent software allowed it to obtain the parameters of pressure and drag present in the surface of the column, and these values were used as a criterion to analyze the performance of different cross sections. The model was validated by comparison with the results from other authors in order to guarantee reliability to the study. The values obtained for different cross sections were compared to standardized values recommended by the Brazilian code NBR 7187/2003, when available.

Keywords. *Columns, drag force, numerical modelling, computational fluid dynamics (CFD).*

Introduction. The first long span bridges reached Brazil around 1850 but only gained importance during the 1930s. In 2011, the survey of the Department of Public Works of the city of Petrópolis-RJ found that about 20 bridges were damaged or destroyed as a result of the elevation of the water level in rivers and streams. According to Rio de Janeiro state government, it took R\$ 110 million to recover bridges throughout the region (1). In 2014, the National Department of Transport and Infrastructure (DNIT) invested R\$ 5.8 billion, with the support of the World Bank, to recover 2,500 bridges on federal highways throughout the country (2). The values involved in these interventions suggest that any measure to improve the performance of these bridges will have a significant economic impact, especially if these measures are taken while the bridges are still being designed. This will also contribute to increase the safety of such structures.

Currently in Brazil the structural project of concrete bridges are based on the recommendations of NBR7187/2003 - "Design of reinforced concrete and prestressed concrete bridges". This code allows the replacement of dynamic loads by static ones majorated by a coefficient. In the case of hydrodynamic loads this coefficient is determined according to the geometry of the column, which can be either rectangular or circular since these are the two most common cross sections of bridge columns (3). Therefore, it is reasonable to assume that the current recommendations presented by NBR7187/2003 may not adequately take into account the diversity of variables existing in the



phenomenon of fluid-structure interaction for the accurate determination of hydrodynamic forces that will occur in the bridge substructure.

Furthermore, Computational Fluid Dynamics (CFD) has seen significant development advances in recent years that have been applied to all areas of Engineering (4). According to Rodrigues (5), the use of CFD has innumerable advantages, such as relatively low cost when compared with the costs of laboratory experiments; agility in obtaining and analyzing results; the ability to simulate real and also ideal conditions; the analysis of a large number of regions of interest in the flow and the creation of a complete set of flow parameters. However, according to Oliveira (6), the use of this tool can also have its disadvantages, such as the limitation of the validity of the mathematical/physical model that will be adopted in the resolution and the existence of problems that do not have adequate mathematical models.

Therefore, studies that seek to find new ways to accurately determine hydrodynamic loads or even contribute to reducing the incidence of this kind of load in structures, have great relevance today, since natural phenomena are difficult to control and computational modeling of flow phenomena is not yet common in engineering offices.

To make a contribution to the research in this area, this work computationally simulates a flow interacting with bridges' columns in several cross-sections, making it possible to obtain a better understanding on how these cross-sections contribute to the existence and intensity of hydrodynamic loads. For this purpose, the main geometries of the columns of bridges in the state of São Paulo that cross medium and large rivers, according to the classification of the Department of Water and Electricity (DAEE), were identified and some proposed geometries were investigated in order to compare their performance with the geometries more commonly used. Both the proposed and existing geometries were modeled in the ANSYS Fluent software, so that it was possible to obtain the hydrodynamic action on the columns and thus determine which one presents the best performance. In addition, the results obtained by the simulation and those from the recommendations of NBR7187/2003 were compared.

Hydrodynamic forces due to a water flow. The rivers of interest for this work were identified through their hydric availability (m^3/s) according to the National Water Resources Information System of the National Water Agency (ANA) (7).

Table 1. Hydric Availability

River	Availability (m^3/s)
Mogi-Guaçu	10 – 100
Paraíba do Sul	> 500
Paranapanema	100 – 500
Pardo	10 – 100
Piracicaba	100 – 500
Tietê	100 – 500



After choosing the rivers, the website of the DAEE (8) was consulted and the maximum historical flow rates of the rivers and the cross-sections of their beds were obtained, so that it was possible to determine the critical flow velocity. According to Mays (9), the critical height of the water depth can be determined from Eq. 1:

$$y_c = \left[\frac{Q^2}{(b^2 g)} \right]^{1/3} \quad (1)$$

where y_c = critical depth; Q = flow; b = channel width; and g = gravity acceleration.

With the critical height it is possible to calculate the flow area and thus obtain the speed using Eq. 2:

$$v = \frac{Q}{A} \quad (2)$$

where v = water velocity; Q = flow; and A = channel area.

In Table 2 it is shown the summary of the information of the chosen rivers.

Table 2. Summary of maximum flow rates

River	Prefix (DAEE)	Flow (m ³ /s)	Section (m ²)	Velocity (m/s)
Mogi-Guaçu	5C-025	1189.27	257	4.63
Paraíba do Sul	1D-008	809.09	199	4.06
Paranapanema	6E-001	2037.17	326	6.26
Pardo	5B-001	2163.97	475	4.55
Piracicaba	4D-007	1418.64	288	4.92
Tietê	7C-003	3624.75	1101	3.29

These rivers constitute a large part of the São Paulo water network and it will be adopted as the basis for this work. The calculated velocity found will be used later during the flow simulations.

Brazilian Code NBR 7187/2003. The efforts that arise as a result of the type of flow and column geometry can be approximated by Eq. 3, which calculates the pressure due to the water in motion, according to NBR 7187/2003.

$$p = k v_a^2 \tag{3}$$

where p = equivalent static pressure; v_a = water velocity; and k = dimensional coefficient.

However, k only has values for circular ($k = 0.34$) or rectangular geometries, varying according to the flow incidence, as shown in Table 3.

Table 3. Values of k as a function of the angle of incidence

Incidence Angle	k
90°	0.71
45°	0.54
0°	0

For other geometries, NBR 7187/2003 recommends: “[...] For elements with other cross-sections, consult the specialized bibliography. [...] The dynamic effect of waves and moving water must be determined using hydrodynamic methods”.

Flow Characterization. When studying a fluid, it is necessary to consider the type of flow to which the fluid is subjected. According to Porto (10), open channel flow regimes can be calculated and classified according to the parameters established by the physicist Osborne Reynolds, using the coefficient named after him as Reynolds number, which can be determined by Eq. 4:

$$Re = \frac{v D_H}{\nu} \tag{4}$$

where D_H = hydraulic diameter; v = fluid mean velocity; and ν = kinematic viscosity.

As previously described, there are different flow patterns that are characterized by the Reynolds number, which according to Rodrigues (11) is “a dimensionless parameter that translates
doi.org/10.32640/tasj.2022.1.45

the effects of viscosity and allows the distinction between the different existing types of flow”. The main factors that depend on the fluid-structure interaction are the formation of vortexes and the consequent generation of forces that interfere with the stability of the columns interacting with the flows. The disturbances present in the flow can change the Reynolds number range, however, in general, the flow patterns can be divided into: laminar, transition, and turbulent.

The flow around a column creates two distinct regions: the main one, called approach flow, and a secondary one, dictated by the viscous characteristics (12). For the study of bridges, the main type of events that occurs are dynamic.

In the case of a response problem in the time domain, the most common example is buffeting, characterized by the forced vibration regime caused by vortexes upstream of the structure. This phenomenon is difficult to model since vortexes can occur randomly or periodically leading to resonance.

In the case of dynamic stability problems, the most common example is flutter, characterized by the joint action of flexion and torsion efforts, with a dynamic response dominated by torsional vibrations. It differs from buffeting in that it manifests itself from a critical flow velocity and because it depends more on the geometry of the structure. As a consequence of the change in the pressure field, it is possible to observe an increase in the level of the free surface upstream of the column and the formation of a winding surface (13).

Solid bodies, in fluid mechanics, can be classified according to their geometric shape as robust or aerodynamic. The robust bodies produce a high drag coefficient, mainly due to the premature detachment of the boundary layer, resulting in the formation of a relatively wide trail. The aerodynamic shapes, on the contrary, delay the detachment of the boundary layer, minimizing the drag coefficient and often producing a high value of the lift coefficient, as occurs on the wings of an aircraft.

According to Coelho (14), “with the appearance of vortexes and forces between the flow and obstacle, dimensionless coefficients appear that relate these same forces that appear in the flow”. Thus, it can be defined:

- a) Lift coefficient: lateral force that acts on the structure in the direction perpendicular to the flow direction and is measured per unit length of the structure.
- b) Drag coefficient: associated with the longitudinal force that acts on the structure and that in general is a component of the total force that acts on the structure in the flow direction. The drag force arises due to the combined effect of the tension on the wall and the pressure force.

This longitudinal force acts on the surface of a body immersed in a moving fluid and is a dynamic force resulting from pressure (normal to the surface) and shear (tangent to the surface) forces. The component of the total force exerted by the fluid on the solid, in the direction of the flow is called drag. The drag force acting on a body is, therefore, composed of two parts: one due to friction (or surface) drag and the other due to pressure (or shape) drag.



The drag force acts in opposition to the direction of movement of the body that moves in the fluid. Its intensity depends on the size, shape, and position of the body, velocity, density and temperature of the fluid. There are three types of drag force: surface drag, which is directly related to the viscosity of the fluid and the surface roughness, wave drag, and shape drag, which is the object of interest in this work.

According to Silva (15), the drag coefficient can be obtained using a mathematical methodology based on the application of the amount of movement in integral form for a control volume, which can be expressed in a simplified way by Eq. 3:

$$C_d = \frac{2F_d}{\rho A v^2} \quad (5)$$

where C_d = drag coefficient; F_d = drag force; ρ = mass density of the fluid; and A = reference area.

Alternatively, White (16) states that the actual pressure distributions of the laminar and turbulent boundary layer are naturally different from those predicted. The laminar flow is very vulnerable to the adverse pressure gradient at the rear of the cylinder and the separation occurs at $\theta \cong 82^\circ$. The wide trail and the very low pressure in the laminar separation region causes a drag coefficient in the order of $C_d = 1.2$. The turbulent boundary layer is more resistant due to the energization caused by the turbulence, which transports energy from outside to inside the boundary layer and thus it resists a little more to the adverse pressure gradient, and the separation is delayed up to $\theta \cong 120^\circ$, causing a narrower trail, higher downstream pressure and a 75% lower drag coefficient, $C_d = 0.3$. This explains the sudden drop in the drag coefficient during the flow regime transition (17).

Numerical modelling. The complexity and the high number of calculations involved in the analysis of dynamic mechanical problems require the use of computational techniques for their resolution and are of fundamental importance, so much that currently researches in these areas are mainly focused on the development of computational models based on numerical methods.

Fluid-structure interaction (IFE) problems are very common, appearing in different areas of engineering. In the case of civil engineering, there are the cases of winds on structures, flows in channels and spillways, water interacting with dams and offshore structures. In the last decades, it has become possible to design increasingly slender and flexible structures capable of withstanding large displacements without reaching rupture. However, if there are interactions with a fluid medium such structures can show effects that are often not foreseen or that are inappropriately considered during its design. Nowadays, it is known that for a more refined analysis of the effects of fluids on structures it is necessary to account for the effects caused by the solid and the fluid in



a coupled way. This is what motivated the emergence of CFD (Computational Fluid Dynamics) based models (18).

In the study of water bodies through computational modeling there will be situations in which certain structures are part of the modeling domain. An example of this is the case of bridge columns, which should be considered in modeling for hydrodynamic analysis. The inclusion of the effects of the columns in the computational modeling can be accomplished through several techniques and models, each of which presents a series of advantages and disadvantages that must be taken into account according to the results to be obtained (19).

Among the main advantages of using CFD, the possibility of solving complete differential equations stands out, making the flow analysis closer to reality and allowing a more detailed study of some specific terms that appear in the governing equations of the problem. Another advantage is the ability to simulate flows in conditions that would not be reproducible in experimental tests, for example, in very large or dangerous scenarios that cannot be simulated experimentally.

A relevant point when numerically analyzing viscous flows are the effects of vorticity in turbulent flows. The Navier-Stokes equations can in principle simulate both laminar and turbulent flows (20). However, the direct simulation of the Navier-Stokes Eq. is a complex and very time-consuming task, being limited to flows with low Reynolds number.

For turbulent flows, where the Reynolds number is very high direct resolution of the Navier-Stokes Eq. is not feasible, which is why alternative methods have been developed. The methods usually are divided into two large groups: Reynolds Averaged Navier-Stokes (RANS) and Large Eddy Simulation (LES). The Direct Numerical Solution (DNS) is based on solving equations without using averages or approximations. In Table 4 these three methods are compared.

In this work the flow to be simulated will have a high Reynolds number, making it a problem not suitable to address using a DNS flow model (which would present the most accurate result). Therefore, in order to obtain the data as a function of time it will be adopted here a RANS based model.

Table 4. Numerical modelling methods

DNS Direct Numerical Simulation	LES Large Eddy Simulation	RANS Reynolds Averaged Navier-
Modeling all time and space scales of turbulence	Generalizes smaller scale movements	Models the average of variables
Time-consuming and expensive simulations	Applicable to larger numbers of Reynolds	Divided into calculation subgroups
In practice, only applicable to low Reynolds numbers	Solves Navier-Stokes equations only for larger scales	Simplified modeling
	Requires finer mesh near walls	



RANS based models. Models based on RANS cannot solve all the turbulence scales. On the other hand, the solution adopted here will model all scales as a single averaged scale, which represents the whole turbulence.

There are several RANS models, according to how Reynolds stresses are obtained. Among these we can highlight the model of two equations, so-called because it uses two scalar quantities, usually turbulent kinetic energy and its dissipation. This method is the most complex and the one with the greatest capacity to model turbulence.

In this work it was used the turbulence model SST (Shear Stress Transport), which is composed of the models of two equations k - ε and k - ω . These three methods are presented in the following.

- a) **Standard k - ε model:** This model of two equations is used in several applications since it presents a good balance between precision and robustness. It consists of two differential transport equations, the turbulent kinetic energy k and the turbulent kinetic energy dissipation rate per unit mass (ε). This model is only valid for totally turbulent flows, where the viscous molecular effects can be minimized. In the regions close to the surface intense gradients appear, demanding a certain degree of refinement of the domain and, as a result, the required computational effort is increased.
- b) **k - ω model:** This model introduces in the constitution of the differential transport equations the energy dissipation rate per unit of volume and time (ω), also referred to as the average frequency, instead of ε . It is a much more cohesive model compared to the standard model k - ε when it comes to regions close to surfaces, in addition to not requiring specific formulations for low Reynolds numbers. It also presents a refinement of the problem domain that demands a lower element density when compared to the k - ε model. However, it also has limitations in the regions farthest from the wall area which can result in significant variations in the results. The solution to circumvent the limitations of these models is to use a combination of equations of the k - ω model for regions close to the wall, and to use equations of the standard model k - ε for regions further away from the wall.
- c) **Shear Stress Transport:** As this model is not a “new model”, but the conjunction of the two previous models, it does not present any new set of equations, but two sets of transport equations, one used for the regions closest to the wall and the other for the farthest areas. The emergence of this new formulation made it possible to predict with greater precision the beginning and the magnitude of the flow separation under pressure gradients in unfavorable conditions as a result of the involvement of the transport effects in the definition of the turbulent viscosity model. In this model, the transport equations for k - ω are most used in the region close to the wall, while the transport equations for k - ε are adopted in the outer region. As previously mentioned, this model appears to address the deficiencies of the other models in relation to variations and poor estimates of parameters. However, in flows where the Reynolds



number is considerably low, the treatment of the simulation in the wall area can be done using just the $k-\omega$ mode.

Simulation procedure. In this work the Finite Volume Method (FVM) was adopted for numerical simulations, since ANSYS Workbench, which is the software chosen for the computational analysis, uses it for modeling. This software has application in several branches of engineering and includes a vast set of essential tools for the implementation of analyzes using CFD.

The application of FVM is based on the integral form of the mass conservation Eq.. The solution domain is divided into a finite number of continuous control volumes and the conservation Eq. is applied to each one. In the centroid of each control volume a computational node is located in which the values of the variables involved are calculated (21). This method can be used in several geometries with structured or unstructured meshes, which leads to robust schemes. A special feature is the fact that this method conserves the numerical flow from one cell to its neighbor, making it a very important method for modeling problems where the flow assumes particular relevance. FVM can be applied to any type of mesh, so it adapts to complex geometries. The mesh defines only the boundaries of the control volume and does not need to be related to a coordinate system.

When applying the FVM, there must be a good balance between the processing time and the accuracy and quality of the results, which leads to not refining the entire mesh but only in regions where there are large variations in the parameters of interest. Therefore, it is necessary to refine the mesh in the region close to the column (area of interest in the analysis) in order to improve the accuracy of the LES model and guarantee the quality of the result.

This work focuses on the study of the interaction of a three-dimensional flow around a column. To perform the simulations a computer with an Intel Core i7 processor with 2.4 GHz, 8 Gb of RAM and with a data storage capacity of 500 GB was used. The simulations will often require computers with a high capacity for data processing, especially when dealing with turbulent flows and three-dimensional modeling.

For the flow definition, a model with the shape of a parallelepiped was adopted, inside which an opening that represents the column under study is inserted. The order of magnitude of the dimensions of the models created will be 25.0 m long, 10.0 m wide and 2.0 m high.

For mesh generation the Ansys Sizing menu was used to work with the components of the solid and applying configurations aiming to obtain the mesh without obstructions. Then, the plans were named so that, when imported into Setup, it auto-configures the entrance and exit of the flow. An example of the generated mesh is shown in Fig.1.

After modeling the problem geometry and performing the mesh generation, the choice of the turbulence model is made. Ansys Fluent was used to process the numerical solving of the problem. It allows numerous conditions necessary for the simulation to be defined, thus allowing the modeling of the most varied types of flow.

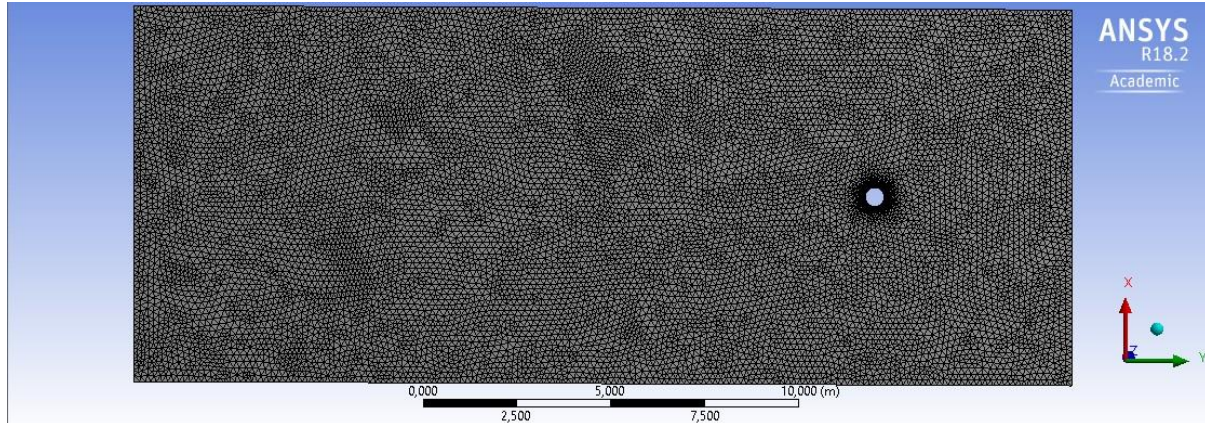


Figure 1. Mesh example

Fluent uses the method of finite volumes (FVm) and CFD codes that contain numerical algorithms for solving Navier-Stokes equations with variables defined at the center of each control volume. To solve the system of equations resulting from the parameters entered the basic options must be configured in the general menu where some characteristics of the simulation are defined, such as the geometry scale, the mesh quality check or the type of the solution method. The numerical resolution of the system of equations in Fluent was carried out using the pressure-based mode most suitable for incompressible flows and the flow was considered Transient. After the resolution it is possible to post-process the results obtained through various tools, such as graphs, videos, histograms, reports, among other options.

In most simulations of real flows, the surface is considered to be a free surface and it is necessary to define the boundary condition of this flow area. The free surface can be considered as a frictionless wall in which the acting pressure is zero, thus simulating the free surface at atmospheric pressure. The column should have its boundary condition defined as a stationary wall.

The software allows the choice of some solution methods, the separation models and some variables that can somehow affect the convergence of the simulation and its respective result. The adopted solution method was the PISO scheme (Pressure-Implicit with Splitting of Operators) which performs two additional calculations related to pressure correction, and takes into account the quality of each mesh element used in the calculation. Therefore, this scheme allows achieving convergence with greater speed and efficiency reducing the simulation processing time. Still, in the simulation processing phase it is necessary to analyze the control of the solution. In this way, the Fluent user guide suggests using as a convergence criterion that the total value of the residuals is less than $1e-6$.

To complete the analysis, it is necessary to define the method to be used in the interpolation of the values obtained for the pressure and velocity fields. According to the Ansys Workbench User's Guide there are three possibilities for this: Hybrid Boot, the Standard Initialization and the

Full Multigrid Initialization (FMG). Hybrid initialization is an ANSYS Fluent initialization method that solves the Laplace Eq. to determine the velocity and pressure fields. All other variables will be corrected automatically based on the mean values of the domain or some form of specific interpolation. This method is the standard for single phase steady-state flows. The time step also assumes particular importance in the resolution since the smaller it is the more accurate the simulation solution will be. However, a very low time step value will imply greater effort and a consequent increase in the simulation time.

Results analysis. In this item the results obtained and the parameters adopted will be presented such as model dimensions, respective boundary conditions, the choice of the turbulence model, and the choice of the solution method.

The differences between the results of the various simulations carried out are due to the different geometries adopted for the columns, more specifically to its cross section. A gradual change of geometry was adopted starting with the square shape and ending with the circle. The simulations whose cross-sections of the columns are circular and square allowed to validate the numerical simulation by comparison with the values presented by other authors.

Regarding the shape of the model the domain will be identical for all simulations varying only the cross-section of the columns. Thus, for example, for a 0.50 m columns, 5.0 m away from the flow entrance, the other dimensions will be 25.0 m long, 10.0 m wide and 2.0 m high. These dimensions follow the recommendation of Azevedo (17) for the proportions of the problem domain in relation to the column diameter. The geometries chosen to be tested are shown in Table 5.

Table 5. Proposed cross sections

Geometry	Figure	Height (m)	Length (m)
(1) Square		0.50	0.50
(2) Parallelogram		0.50	1.00
(3) Oblong		0.50	1.50
(4) Elliptic		0.50	1.00
(5) Circular		0.50	0.50

Regarding the design of the mesh for each simulation this was done based on the process presented in item 4 of this work. Regarding the constituent materials, the materials inherent in all simulations are water as a fluid material and aluminum (the standard Fluent option) for the solid material, since its constitution has no influence on the result of this study and the real column can always be coated with a specific material, if necessary. The water has a density of 998.2 kg / m³

and a dynamic viscosity of 1.003×10^{-3} . Following the information presented for the rivers' flows (Table 2), a speed of 6.26 m/s was adopted, which results in $Re = 2.19 \times 10^7$, classified as turbulent regime. The boundary conditions are the same for all simulations and in the present study there are five types of boundaries: entry, exit, free surface, solid surface and symmetry.

In the columns the boundary condition Wall was defined which makes all velocity components null and transforming it into an obstacle for the flow. In the channel exit section, the free exit condition was used, defined in the Fluent code as Outflow, without the need to impose values on any variable. The riverbed was defined as Wall in the same way it was defined for the columns. In turn, the lateral boundary conditions were defined as Symmetry, a boundary condition that forces the flow variables to be symmetric about a plane parallel to the flow. The choice of this boundary condition for the side walls aimed to guarantee the absence of wall effects in the flow. Regarding the solution method chosen for all simulations the one adopted was PISO due to the specifications presented previously. The characteristics described in this item are common to all simulations performed in this work. In the sequence, only the particular characteristics of each one is addressed, specifically the simulation time and the shape of the cross sections of the columns.

Simulation 1. Column with square cross section. In this simulation, 20 seconds of flow were simulated which required about 25 minutes of data processing. The introduction of an obstacle in the flow causes the velocity of its particles to change and Fluent allows to have a general insight in this case through the top view of the flow velocity and the corresponding pressure distribution (Fig.2). It can be seen that the maximum pressure acting on the column is 32.2 kPa and 23.9 kPa.

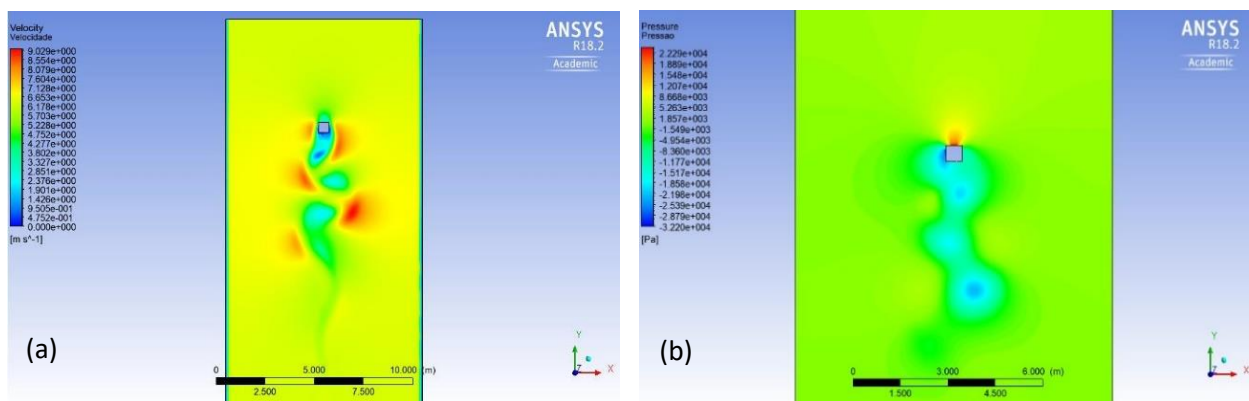


Figure 2. Column 1 – top view of the flow (a) velocity and (b) pressure

Simulation 2. Column with cross-section in the form of a parallelogram. In this case 20 seconds of flow were simulated, which required about 32 minutes of data processing. It can be seen that the maximum pressure acting on the column is 23.77 kPa and 17.13 kPa (Figure 3).

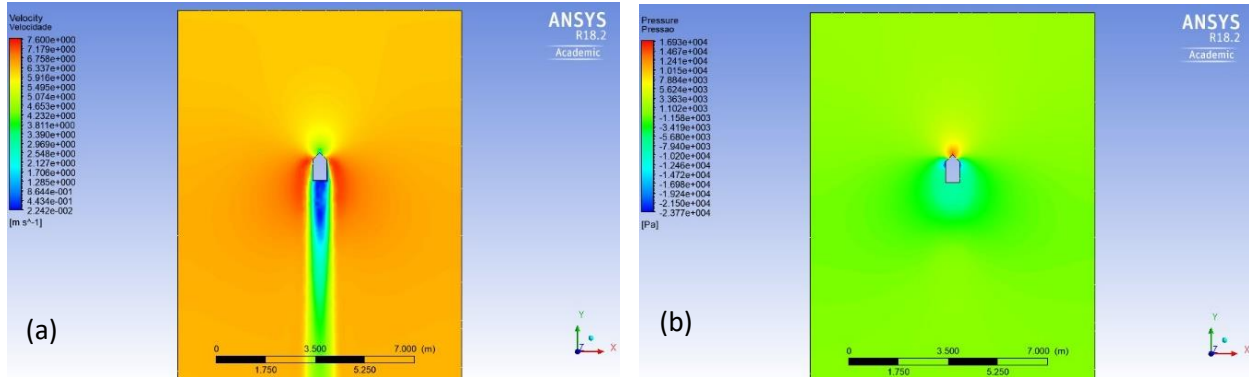


Figure 3. Column 2 – top view of the flow (a) velocity and (b) pressure

Simulation 3. Column with oblong cross-section. In this simulation 20 seconds of flow were simulated, which required about 25 minutes of data processing. It can be seen that the maximum pressure acting on the column is 33.84 kPa and 18.15 kPa (Figure 4).

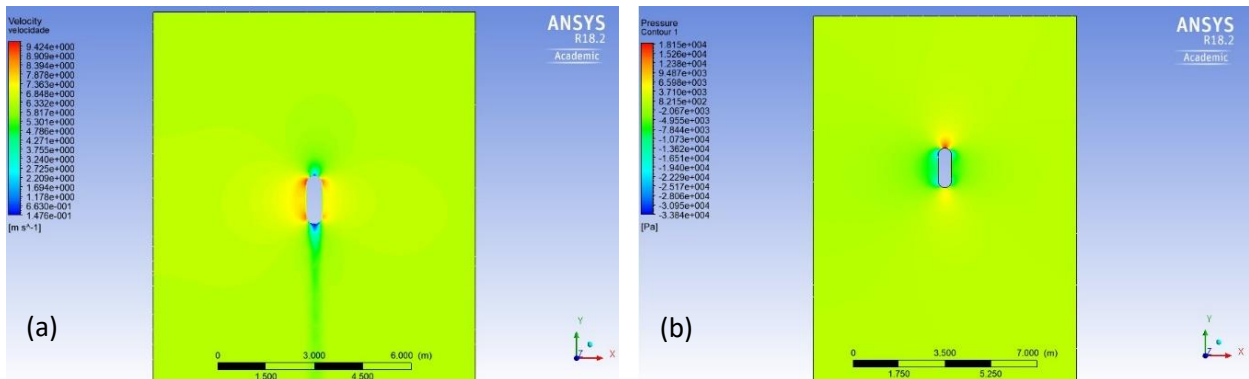


Figure 4. Column 3 – top view of the flow (a) velocity and (b) pressure

Simulation 4. In this simulation, 20 seconds of flow were simulated, which required about 25 minutes of data processing. It can be seen that the maximum pressure acting on the column is 34.95 kPa and 17.93 kPa (Fig.5).

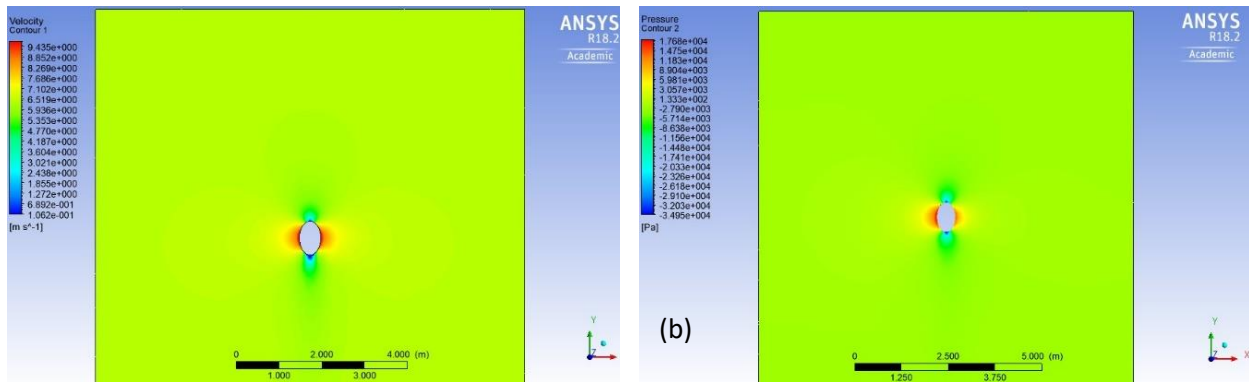


Figure 5. Column 4 – top view of the flow (a) velocity and (b) pressure

Simulation 5. Column with an elliptic cross-section. In this simulation 20 seconds of flow were simulated, which required about 25 minutes of data processing. It can be seen that the maximum pressure acting on the column is 38.0 kPa and 18.5 kPa (Figure 6).

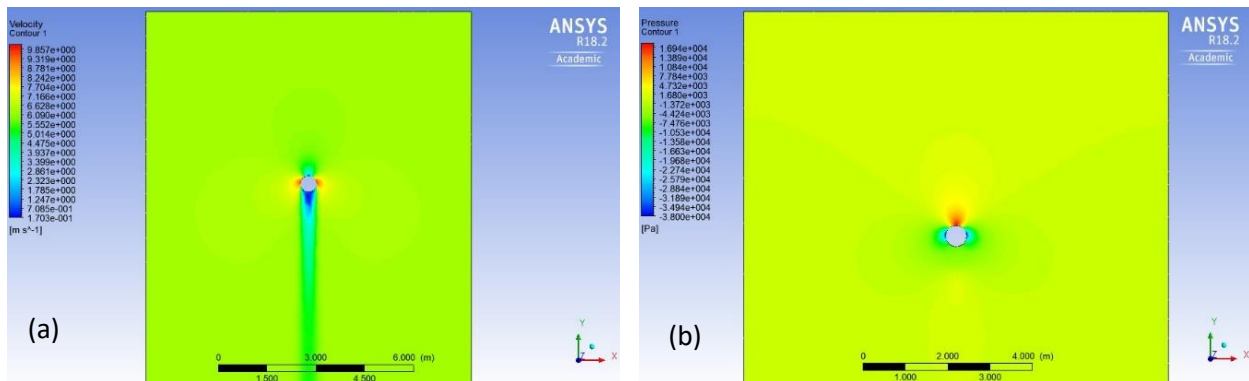


Figure 6. Column 5 – top view of the flow (a) velocity and (b) pressure

Discussion. After obtaining the results the numerical model was validated by comparing the values obtained with those found by other authors and also with NBR 7187/2003. These comparisons are presented in Table 6.

Table 6. Model Validation

References	Values	Drag Coefficient (C_d)	
		Square	Circular
This work	C_d	1.03	0.37
	C_d	1.07	0.3



White	Error (%)	4%	-23%
José	C _d	1.05	0.47
	Error (%)	2%	21%
ABNT	C _d	0.93	0.5
	Error (%)	-11%	26%

It is necessary to emphasize that the definition of theoretical drag coefficients is not common to all authors and for each case it is necessary to adapt and compare results with different coefficients. So, according to Yonis (22), for a turbulent flow around a column with a square section with average drag, it is 2.199. For a circular column cross section, Dong (23) suggests the drag coefficient of 1.143 and for Gopalkrishanan (24) the value is 1.186, while Fornberg (25) suggests 1.49 and Ding (26) 1.71. A possible reason for these variations could be the different Reynolds numbers adopted by the authors since all of them present the coefficient considering only $Re > 104$, but without specifying the real value employed.

One of the objectives of this study is to compare the value of the simulations for columns of square and circular sections with the respective values obtained using the coefficients suggested by NBR 7187/2003. The results are presented in Table 7. Eq. 5 was used to calculate the standardized values. It can be seen that the standardized values for the square geometry with perpendicular flow incidence is within the simulated range. The circular section showed a lower result than the simulation interval.

Table 7. Comparison between pressures

Pressure	Square Section		Circular Section	
	NBR 7187/2003	Numerical	NBR	Numerical
Minimum (kPa)	27.80	23.90	13.30	18.50
Maximum (kPa)		32.20		38.00

Another comparison that must be done is between the drag force values of the five simulations with the purpose of obtaining the more efficient geometry for the reduction of this force intensity. Thus Table 8 shows the values obtained in an ascending order and the efficiency of each section in comparison to the value of the square cross-section column.

The most efficient case is the elliptical cross section. It can be noticed that the geometries with curved faces present a better performance. This occurs because the effect of the incident flow is reduced due to the smoothness of its contour. The analysis of the turbulence associated with each case also showed that the geometries that have a length to width ratio greater than 1 tend to have a smaller tail as the ratio grows, or in other words, they tend to have less turbulence.

Tabela 8. Simulated drag forces values

Shape	Section	Drag Force (N)	Efficiency (%)
Elliptic (4)		574.94	97%
Oblong (3)		1593.57	92%
Circular (5)		3651.31	82%
Parallelogram (2)		8393.25	58%
Square (1)		20130.25	0%

Conclusions and future work. In this work several types of column cross-sections were studied to determine which would be more efficient in reducing the drag force on it due to a water flow. From the obtained values it can be seen that columns with an elliptical section give more rise to lower drag forces than other sections, and the reduction of this force in relation to a square section is 97%. However, it is necessary to emphasize that it is also important to take into account the resistant capacity of the column in relation to the shape of its cross-section, and in this way, it appears that the oblique section presents itself as an interesting alternative because it is easy to perform, has a high-efficiency rate, and in addition also has a high rigidity to resist the action of the drag force.

It is also possible to improve the efficiency of the sections without adopting cross-sections that may be difficult to construct, by installing elements of hydrodynamic form upstream and downstream of the column in order to smooth the flow passage and decrease the drag force. This solution can also be applied as a low-cost intervention to columns already existing in rivers with a history of high-water levels, in order to avoid effects not foreseen during the bridge design.

The results obtained in this work are relevant not only from an economic point of view but also from the perspective of the bridge's safety which justifies the continuity of research in this area. In this sense, it is of interest to analyze the flow around structures with more complex sections; the analysis of the influence of geometry on soil erosion at the base of the column; testing new turbulence models; the realization of new simulations with specific meshes in the areas where vortexes or other phenomena relevant to the flow occur. Such research will contribute to a better understanding of the phenomena involving the emergence of drag forces in bridge columns and can provide new criteria for the design of this type of structure that will make them more economic and safer.

Author contributions: Clemente THM: computational simulations, writing; Campos NBF: supervision, writing.



References.

- (1) Terra Networks Brasil S.A. RJ: depois de enchente, Petrópolis começa a receber pontes. Terra. 2011 Feb 02; Available from: <https://www.terra.com.br/noticias/brasil/rj-depois-de-enchente-e-petropolis-comeca-a-receber-pontes,7cca44fa607da310VgnCLD200000bbcceb0aRCRD.html>.
- (2) Governo Federal do Brasil. Governo aprova projeto de recuperação de 2,5 mil pontes e viadutos. Governo Federal. 2011 Jan 11; Available from: <https://www.gov.br/infraestrutura/pt-br/assuntos/noticias/ultimas-noticias/governo-aprova-projeto-de-recuperao-de-25-mil-pontes-e-viadutos>.
- (3) Associação Brasileira de Normas Técnicas. Design of reinforced concrete bridges and prestressed concrete – Procedure, NBR 7187. 2003; Rio de Janeiro, Brasil.
- (4) Fernandes JWD. Fluid-structure interaction with incompressible flows using finite element method [dissertation]. 2016; Dep. Structures, Univ. São Paulo, São Carlos, Brazil.
- (5) Rodrigues JML. Study of the influence of the cross-section of the pillars the drag force [dissertation]. 2012; Univ. Beira Interior, Covilhão, Portugal.
- (6) Oliveira PJSP. Mecânica Computacional. Notas didáticas. 2001; Univ. Beira Interior, Covilhão, Portugal.
- (7) ANA-Agência Nacional de Águas. Água Superficial. Sistema Nacional de Informações sobre Recursos Hídricos. 2022; Available from: <http://portal1.snirh.gov.br/ana/apps/webappviewer/index.html?id=3a78c627739e448f8ea7e3e6aa9b7a1b>.
- (8) DAEE Departamento de Água e Energia Elétrica. Banco de dados fluviométricos por curso d'água. Banco de dados hidrológicos. 2022; Available from: <http://www.hidrologia.dae.sp.gov.br/>
- (9) Mays LW. Hydraulic Design Handbook. 1st ed., Ed. Mcgraw-Hill, New York, USA. 1999.
- (10) Porto R M. Hidráulica Básica. 4th ed., Editora EESC-USP, São Carlos, Brazil. 2006.
- (11) Fox RW, Pritchard PJ, McDonald AT. Introduction to Fluid Mechanics. 8th ed. John Wiley & Sons Inc, Danvers, USA. 2011
- (12) Ramos PX, Pêgo JP, Maia R. Numerical simulation of the flow around a pier. 2021 Oct 01; 7^{as} Jornadas de Hidráulica, Recursos Hídricos e Ambiente, FEUP, Porto, Portugal. 2021;70-8.
- (13) Cardoso AH. Erosões localizadas junto de esporões fluviais e de encontros e pilares de pontes [dissertation]. FEUP, Porto, Portugal.1998.
- (14) Coelho JFL. Desenvolvimento de uma instalação experimental para estudo de fenómenos de interação fluido-estrutura [dissertation] Univ. Federal do Rio Grande, Porto Alegre, Brazil, 2008.
- (15) Silva CRI, Vieira EDR, Determinação experimental do coeficiente de arrasto para o escoamento ao redor de esferas utilizando o método de integração da pressão e o balanço da

quantidade de movimento. XII Cong. Nac. de Estudantes de Eng. Mecânica. 2005 ago 22-26. Ilha Solteira, , UNESP, Ilha Solteira, Brazil.

(16) White FM, Fluid Mechanics, 7th ed., New York, USA, Ed. Mcgraw-Hill. 2011.

(17) Azevedo MACS. Estudos preliminares sobre ejeção de vórtices em torno de um cilindro no regime turbulento com separação laminar [dissertation]. FEUP, Porto, Portugal. 2011.

(18) Zanutto CP. Aplicação de técnicas de Fluidodinâmica Computacional (CFD) na avaliação da hidrodinâmica e da transferência de massa em estágio de coluna de destilação [dissertation], Centro Ciências Exatas, UFSCar, São Carlos. 2015.

(19) González-Gorbeña E, Rosman PCC. Sobre a Modelagem Computacional de Estruturas Imersas em Escoamentos em Escala Subgrid. RBRH, 2016 jan./mar; 21(1):209-21. (DOI: 10.21168/rbrh.v21n1)

(20) Teixeira PRF. Simulação Numérica da Interação de Escoamentos Tridimensionais de Fluidos Compressíveis e Incompressíveis e Estruturas Deformáveis Usando o Método de Elementos Finitos [Ph.D. thesis], PPGEC, UFRGS, Porto Alegre, Brazil. 2001.

(21) Gonçalves N. Método dos Volumes Finitos em Malhas não estruturadas [dissertation], Faculdade de Ciências, Univ. do Porto, Porto, Portugal.2007.

(22) Younis BA, Przulj VP. Computation of turbulent vortex shedding. Comput. Mechanics. 2006; 37(5):408–25. (doi: 10.1007/s00466-005-0713-2)

(23) Dong S, Karniadakis GE. DNS of flow past a stationary and oscillating cylinder at $Re=10000$. Journal of Fluids and Structures, 2005 Mai; 20(4):519-31. (doi: <https://doi.org/10.1016/j.jfluidstructs.2005.02.004>)

(24) Gopalkrishnan R. Vortex-Induced Forces on Oscillating Bluff Cylinders [Ph.D. thesis]. Depart. of Ocean Eng., MIT, Cambridge, Massachusetts,1993.

(25) Fornberg B. A numerical study of steady viscous flow past a circular cylinder. J. Fluid Mech, 1980 Jun 26; 98(4):819-55. (doi: <https://doi.org/10.1017/S0022112080000419>)

(26) Ding H, Shu C, Yeo KS, Xu D. Simulation of incompressible viscous flows past a circular cylinder by hybrid FD scheme and meshless least square-based finite difference method. Comput. Methods Appl. Mech. Eng. 2004; 193:727-44. (doi:10.1016/j.cma.2003.11.002)

Authors ORCID (<http://orcid.org/>)

Thiago Henrique Malandrino Clemente: <https://orcid.org/0000-0001-8225-6306>

Nivaldo Benedito Ferreira Campos: <https://orcid.org/0000-0002-8967-4313>